# MEASURED PERFORMANCE OF BUILDING INTEGRATED PHOTOVOLTAIC PANELS – ROUND 2

**Brian P. Dougherty**
**National Institute of Standards and Technology**
**Gaithersburg, Maryland 20899-8632**

**A. Hunter Fanney, Ph.D.**
**National Institute of Standards and Technology**
**Gaithersburg, Maryland 20899-8632**

**Mark W. Davis**
**National Institute of Standards and Technology**
**Gaithersburg, Maryland 20899-8632**

## ABSTRACT

Architects, building designers, and building owners presently lack sufficient resources for thoroughly evaluating the economic impact of building integrated photovoltaics (BIPV). The National Institute of Standards and Technology (NIST) is addressing this deficiency by evaluating computer models used to predict the electrical performance of BIPV components. To facilitate this evaluation, NIST is collecting long-term BIPV performance data that can be compared against predicted values. The long-term data, in addition, provides insight into the relative merits of different building integrated applications, helps to identify performance differences between cell technologies, and reveals seasonal variations.

This paper adds to the slowly growing database of long-term performance data on BIPV components. Results from monitoring eight different building-integrated panels over a 12-month period are summarized. The panels are installed vertically, face true south, and are an integral part of the building's shell. The eight panels comprise the second set of panels evaluated at the NIST test facility. Cell technologies evaluated as part of this second round of testing include single-crystalline silicon, polycrystalline silicon, and two thin film materials: tandem-junction amorphous silicon (2-a-Si) and copper-indium-diselenide (CIS).

Two 2-a-Si panels and two CIS panels were monitored. For each pair of BIPV panels, one was insulated on its backside while the backside of the second panel was open to the indoor conditioned space. The panel with the backside thermal insulation experienced higher midday operating temperatures. The higher operating temperatures caused a greater dip in maximum power voltage. The maximum power current increased slightly for the 2-a-Si panel but remained virtually unchanged for the CIS panel. Three of the remaining four test specimens were custom-made panels having the same polycrystalline solar cells but different glazings. Two different polymer materials were tested along with 6 mm-thick, low-iron float glass. The two panels having the much thinner polymer front covers consistently outperformed the panel having the glass front. When compared on an annual basis, the energy production of each polymer-front panel was 8.5 % higher than the glass-front panel.

Comparison of panels of the same cell technology and comparisons between panels of different cell technologies are made on daily, monthly, and annual bases. Efficiency based on coverage area, which excludes the panel's inactive border, is used for most "between" panel comparisons. Annual coverage-area conversion efficiencies for the vertically-installed BIPV panels range from a low of 4.6 % for the 2-a-Si panels to a high of 12.2 % for the two polycrystalline panels having the polymer front covers. The insulated single crystalline panel only slightly outperformed the insulated CIS panel, 10.1 % versus 9.7 %.

## INTRODUCTION

One infrastructure hurdle facing the solar energy industry is the difficulty with predicting the installed performance of building integrated photovoltaic (BIPV) components. A few examples of questions that go unanswered include:

· What will be the avoided costs from the on-site electrical power generation?

· What are the tradeoffs from using insulated versus un-insulated BIPV components?

· Does the rank ordering of PV technologies based on rated performance translate to the same rank ordering when applied in a particular field installation?

Such unanswered questions leave the project decision makers – the architects, building designers, and building owners – justifiably uneasy about pursuing a building design that incorporates solar photovoltaic components. These decision makers need more information and better technical

resources in order to fully consider the merits of a particular BIPV project.

Work is underway to correct the current information deficit on BIPV installation options and to provide tools for answering questions like those listed above. One particular area of focus is the validation and refinement (as needed) of computer algorithms that estimate the electrical power generation capabilities of a specific BIPV installation. A few computer models presently exist which predict the electrical power generation of photovoltaic arrays. Researchers at the National Institute of Standards and Technology (NIST) are investigating how well these public-domain algorithms may perform in predicting the electrical performance of BIPV panels. NIST has thus far focused on models published by the Sandia National Laboratories and the University of Wisconsin [1,2, 3], but plans to include additional algorithms that have been reported within the technical literature [4].

In order to use these computer models, a combination of data resources are needed. First, each computer model requires its own unique set of input parameters that define the performance characteristics of each BIPV panel. Examples of these panel-specific parameters include short circuit current, open circuit voltage, maximum power voltage and current at nominal rating conditions, temperatures coefficients, shunt and series resistances, and empirical data on the effects of angle of incidence and air mass. Although values for some of these parameters may be reasonably approximated from the literature or provided by the manufacturer, most are not readily available. As a result, each BIPV panel used in the model validation effort is tested at NIST to determine the needed computer model input parameters. Most of these "model parameter" tests are conducted outdoors using a large, well-instrumented solar tracker. The tests require anywhere from a few hours to the entire sunrise-to-sunset interval to complete. Detailed information on how these tests are conducted, the data that are gained, and past results are provided in references 5 and 6.

The second major set of data needed for validating the computer models is in-situ performance measurements of BIPV panels over a long period of time, preferably a complete year. The electrical power production as a function of time is the main measurement. Electrical current, voltage, and cell and/or backside panel temperatures are also of interest, along with the corresponding meteorological conditions. Finer time steps are preferred because they aid both understanding and modeling instantaneous performance. The lack of long-term BIPV performance data led NIST to construct a test facility to collect such data. The resulting year-long data sets contain a combination of integrated and instantaneous measurements recorded every 5 min. I-V curve traces are available at the same 5 min intervals.

Although the main purpose of the long-term performance data is to evaluate the predictive capability of a given computer model, the data are also informative for demonstrating daily, monthly, and annual performance, and for showing the impact of solar irradiance, panel temperature, and angle of incidence. And when multiple BIPV panels, each having a unique construction, are tested side-by-side, differences between BIPV panel types can be quantified. This paper deviates from the main mission of computer model validation and instead touches on these other informative topics.

Test results from monitoring eight BIPV panels over a complete calendar year are reported. The eight panels comprise the second set of panels evaluated at the same NIST test facility [7]. The panels are installed vertically, face true-south, and are an integral part of the building's shell. Two of the eight BIPV panels tested use tandem-junction amorphous silicon (2-a-Si) cells. Another two panels use copper-indium-diselenide (CIS) cells. For each of these paired panel sets, one was insulated on its backside while the backside of the other panel was open to the indoor conditioned space. Three of the remaining four test specimens were custom-made panels that differed only in their front covers or glazings: one used ethylene-tetrafluoroethylene copolymer (ETFE), the second used polyvinylidene fluoride (PVDF), and the third used 6 mm-thick, low-iron float glass. These three panels used polycrystalline silicon (poly-Si) solar cells. The last test specimen was a hold-over from the first round of testing, a custom-made panel having single-crystalline silicon (mono-Si) cells and a 6 mm-thick, glass front cover.

## TEST FACILITY AND BIPV PANEL DESCRIPTIONS

A BIPV panel installed in the NIST long-term test facility becomes an integral part of the building's wall, a weathering and thermal "insulating" building component. For the Round 2 testing reported here, the facility was partitioned to accommodate eight BIPV panels. The facility includes a meteorological station with, most notably, solar radiation sensors that are installed in the same vertical, true-south-facing orientation as the BIPV panels. An ultrasonic wind sensor is mounted in the facility and provides a local wind speed measurement. A small-size BIPV panel is also installed. This panel is used for quantifying the heat flux through an uninsulated BIPV panel, a topic for discussion in a future technical paper. The BIPV panel layout used during the Round 2 testing is depicted in Fig. 1.

The panels in test stations A to D were custom-fabricated. For all four of these panels, 6 mm glass acted as the structural element. In two cases, the glass was also the front cover and so the built-up layers were glass – EVA[1] – PV cells – EVA – opaque backsheet[2]. For the other two cases, a comparatively thin polymer was used as the front cover, ETFE for the BIPV panel in test station C and PVDF for the panel mounted in test station D. Both polymers have a thickness of 0.05 mm (2 mils). The built-up layers for these two panels were polymer – EVA – PV cells – EVA – opaque backsheet – EVA – glass. The BIPV panels in test stations B, C, and D used 125 mm, square poly-Si cells supplied from the same manufacturer bin and lot. The panel installed in test station A used 125 mm, (rounded) octagonal mono-Si cells. Each of these panels contains 72 series-wired cells. The backside of each of these panels was well insulated using 100 mm of extruded polystyrene during the year-long monitoring period. The junction boxes for these four crystalline silicon solar cell panels – as well as the junction boxes for the four thin film panels – were located on the wall beside each panel; they were not attached to the panel's backside. By remotely locating the junction boxes, the task of adding backside insulation was made easier and any local panel temperature variations created by an attached junction box were avoided.

[1] Ethylene Vinyl Acetate
[2] A laminated product having 3 polymer layers

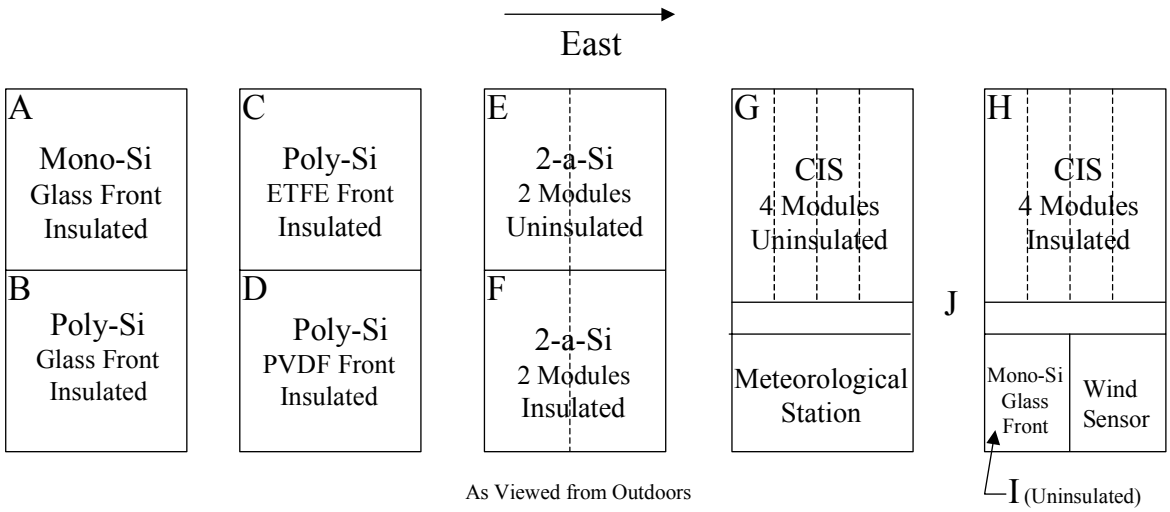


**Figure 1. BIPV Panel Configuration**

The panels in test stations E and F were created using two, tandem-junction amorphous silicon framed modules. At the request of NIST, the manufacturer supplied slightly shortened versions of a production module. The modification allowed the panels to be more readily installed in the NIST long-term test facility. Two custom-length modules were coupled to make a "BIPV panel." The modules were wired in parallel. The 2-a-Si panel in test station F was insulated using 100 mm of extruded polystyrene while the backside of the panel is test station E remained directly exposed to the indoor air.

The PV technology investigated in test stations G and H was copper indium diselenide. Four commercially available modules were combined to make a BIPV panel. The modules were connected in parallel. The CIS panel in test station H was insulated on its backside while the test station G panel was left uninsulated. Additional information about the four PV technologies that were evaluated during the Round 2 testing is provided in Table 1.

An effort was made to avoid top shading and to maximize the midday interval when a panel experienced no side shading (i.e., vertical shadows). The test facility was designed so that the BIPV panels are minimally recessed into the wall. Also, where possible, the BIPV panels are designed to have an inactive top border sufficient to avoid shading along their upper PV edge. (Regrettably, the 2-a-Si panels minimally failed on this pursuit, experiencing a worst-case shadow of 9 mm.) Side inactive borders on the BIPV panels help to lengthen the midday period when the entire PV cell area is unshaded. For the BIPV panel constructed from framed modules – the 2-a-Si and CIS panels – shading caused by this framing plus the framing components of the test facility had to be considered. The borders and recesses associated with both framing elements are included in Table 1.

The 2-a-Si and CIS panels were installed in the long-term test facility between July 31 and August 2, 2001. The test station B, C, and D panels were installed between August 24 and 28. All wiring was completed by August 31. Installation of test station A's panel dates back to September 1999. The Round 2, year-long monitoring began on January 1, 2002. During the months leading up to this start date, the panels were operated for extended periods at both maximum power tracking and at open circuit. With the 4- to 5-month preconditioning period, the year-long performance for the panels, especially the 2-a-Si panels, is representative of stabilized performance.

## DATA MEASUREMENTS

Each BIPV panel is connected to a Raydec, Inc. RD-2400S photovoltaic multi-tracer.[3] The multi-tracer is an integrated measurement system that allows simultaneous testing of multiple photovoltaic products. For our application, the multi-tracer is configured via a computer to independently load and operate each BIPV panel at its peak power point. The multi-tracer samples each panel's current and voltage plus the output signals from thermocouples and a precision spectral pyranometer (PSP). The thermocouples provide the backside temperature of each BIPV panel and the outdoor ambient temperature; the PSP measures the global solar radiation in the same vertical plane as the panels. These samples are made every 15 s with the average values begin saved every 5 min. IV curves are traced at these same 5 min intervals. The multi-tracer otherwise continually monitors and updates, as needed, the loads to maintain maximum power tracking. The rate of such load updates is typically once every second.

A separate data acquisition system tracks meteorological conditions and the BIPV systems' thermal performance. For example, the custom-made panels of test stations A to D were laminated to have two foil-type thermocouples embedded within the panel, at positions directly behind centrally-located PV cells. One of each pair of embedded thermocouples was monitored during the Round 2 testing. For all BIPV panels, this second data acquisition system provided a redundant measurement of backside temperature. For the BIPV panels that were insulated on their backsides – i.e., panels in test

[3]Certain trade names and company products are mentioned in the text or identified in an illustration in order to adequately specify the experimental procedure and equipment used. In no case does such an identification imply recommendation or endorsement by the National Institute of Standards and Technology, nor does it imply that the products are necessarily the best available for the purpose.

**Table 1. Building integrated photovoltaic panel specifications**

| Cell Technology | Single Crystalline (m-Si) | Poly Crystalline (p-Si) | Tandem Junction Amorphous (a-Si) | Copper Indium Diselenide (CIS) |
|---|---|---|---|---|
| Panel Dimensions, W x H (m x m) | 1.38 x 1.18 | 1.38 x 1.18 | 1.33 x 1.18 | 1.32 x 1.29 |
| Nominal Cell Dimensions (mm x mm) | 125 x 125 | 125 x 125 | 1160 x 9 | 1260 x 6.9 |
| Number of Cells (in series) | 72 | 72 | 68 | 42 |
| Number of Bypass Diodes | 4 | 4 | 0 | 4 |
| Adjacent Cell Spacing (mm) | 2 | 2 | — | — |
| Vertical Border Widths (mm) | 100 | 98 | 1.6 & 19[1] | 11 & 28[1] |
| Top Border Width (mm) | 72 | 103 | 3.2 & 19[1] | 9.5 & 48[1] |
| Recessed Distance to Front Cover (mm) | 7.9 | 6.4 | 1.6 & 8.7[1] | 2.4 & 9.5[1] |
| Glazing Covered by PV Cells (%) | 63 | 70 | 94 | 85 |
| Rated Power (W) – NIST | 133 | 143 – 155[2] | 2 x 46.7[3] | 4 x 38.8 |
| Rated Power (W) – Alternative Source | — | 147 - 154[2,4] | — | 4 x 40[5] |
| Total Cell Area ($m^2$) | 1.020 | 1.134 | 1.487 | 1.451 |
| Coverage Area ($m^2$) | 1.160 | 1.168 | 1.487 | 1.451 |
| Aperture Area ($m^2$) | 1.682 | 1.682 | 1.682 | 1.935 |

[1]Shading created by the PV module framing and by the test facility framing were both considered. The distances are listed in the corresponding order.
[2]The first entry corresponds to the panel having the glass front; the second entry applies to the panel having the ETFE front cover. The power for the PVDF panel approached the ETFE value.
[3]This value was determined based on testing completed after approximately 100 h where the 2-a-Si panel was exposed to sunlight and so does not reflect stabilized performance.
[4]Based on flash simulator testing conducted by a third party.
[5]Based on manufacturer published ratings for the particular model of PV module.

stations A, B, C, D, F, and H – a large area heat flux transducer with attached thermocouple were recessed into the face of the foam insulation that abuts to the panel's backside. The meteorological measurements included redundant measurements of the outdoor ambient temperature and the vertical-plane global solar radiation. Others measurements included the indoor ambient temperature plus the effective sky temperatures of both the outdoor and indoor environments – as measured using precision infrared radiometers. The data acquisition system was synced with the multi-tracer, and saved its instantaneous measurements at the same 5 min time steps. Additional information on the instrumented test facility is provided in reference 8.

The multi-tracer and most of the sensors were calibrated prior to initiation of the Round 2 testing. As a continual check of the multi-tracer's integrated power measurements, a dedicated digital power analyzer was connected inline with one of the BIPV panels, the one in test station D. The percent difference between these two measurements of daily energy production typically fell between 0.7 % and 1.2 %.

The electrical performance data are analyzed while considering five different daily intervals. One daily interval was based on the daily sunrise to sunset period. A second interval was selected as times when all eight BIPV panels registered a positive power output. The three other intervals were defined based on the midday period when the 2-a-Si panels, the CIS panels, and the similarly constructed panels in test stations A to D, respectively, experienced no side shading. The duration of the daily data reduction interval for each of the five cases is plotted in Fig. 2 as a function of the day of the year.[4] For comparison purposes, one additional case is included in Fig. 2, a hypothetical flush-mounted panel having no exterior framing components that can cause shading.

Figure 2 shows that the daily data reduction interval varies considerably over the year and from one case to another case. When using the interval where the 2-a-Si panel is unshaded, for example, daily performance is based only on the 2 h that bracket solar noon on the summer solstice while only increasing to a midday interval of 6 h and 25 min on the best day. The interval based on measured power generation slightly

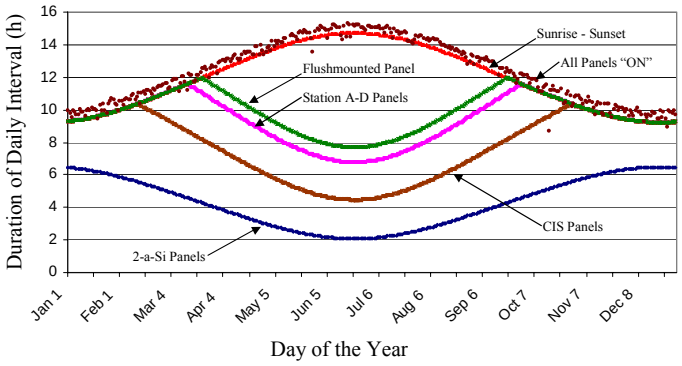


**Fig. 2 Daily Data Reduction Intervals for Six Different Selection Criteria**

[4] The Fig. 2 plots do not account for part-year, early morning shading caused by an adjacent building on the NIST campus. Data collected during these early morning shading periods were excluded from the data analysis.

exceeds the sunrise-to-sunset daily durations, thus reflecting the slightly longer pre-dawn to post-dusk day light interval. The mid-year period where the plot for the hypothetical flush-mounted panel deviates from the sunrise-to-sunset plot is due to the time interval each day when the relative position of the sun is north of the building's south-facing facade. During this period, the incident angle exceeds 90° for a period following sunrise and for an equal period prior to sunset. The difference between the flush-mounted case and the three actual cases below it in Fig. 2 quantifies the effect of the framing used to mount the panels within the building wall or, if present, the effect of the PV module's own framing. These framings delay the end of morning shading and cause the earlier onset of afternoon/evening shading.

The results presented in this paper focus on the sunrise-to-sunset data reduction interval. To help quantify the effect of the chosen interval, results associated with the 2-a-Si interval, the shortest midday span, are interjected.

## ANNUAL, MONTHLY, AND DAILY PERFORMANCE

Six of the Round 2 BIPV panels were insulated on their backsides while the panels in test stations E and G operated with no backside insulation, Fig. 1. Prior to and following the year-long period when this configuration was maintained, data were collected for several weeks, but now with all eight panels having no backside insulation. These baseline periods were mainly used to determine the differences in the paired CIS and 2-a-Si panels under identical operating conditions. From these baseline periods, the 2-a-Si panel in test station F was found to outperform the panel in test station E. Similarly, the performance of the CIS panel in test station H was found to surpass the performance of the test station G CIS panel. In both cases, the differences in power generation correlated relatively well with solar irradiance. For the CIS panels, the relationship was linear. For the 2-a-Si panels, the best fit was that for a second-order, critically damped system. These fits were used to correct each 5 min power reading for the uninsulated test station E and G panels over the year-long period when the other panels were insulated. This correction was made in an effort to single out any effect the backside insulation may have on power generation.

On an annual basis (i.e., year 2002 data), the correction for the CIS panel in test station G caused a 2.1 % and 1.6 % increase to the midday and sunrise-to-sunset energy production values, respectively. The correction to the 2-a-Si panel in test station E amounted to increases of 2.0 % and 4.0 % for the same two data collection intervals. The corrections for the 2-a-Si panel accounted for a performance offset that was more prevalent at the lower irradiances. One possible explanation for the offset is the existence of low energy defects in the junction material of one or both modules used for the test station G panel. At the lower irradiance levels, the excited electrons have a greater tendency to become trapped in shallow defects within the junction material. These defects can be caused by contaminants within the junction material and/or irregularities in the vapor deposition layers [9]. All of the test station E and G results reported below are based on the corrected, 5 min-averaged power values.

Figure 3 shows the annual conversion efficiencies for each of the Round 2 BIPV panels. The plotted percentages are based on 360 d of data and correspond to data collected during the sunrise-to-sunset interval. Efficiencies are plotted based on two different areas, total cell area and the coverage area. Coverage area equals the panel's total area minus any inactive border. For panels constructed using crystalline wafer PV cells, the coverage area includes any separation spacing between adjacent cells plus any voids created by non-rectangular PV cells. Such voids only existed on the mono-Si panel due to its octagonal shaped cells. Because the four panels constructed using thin film materials are continuous laminates having no voids, cell area and coverage area are the same, as are the corresponding efficiencies.

Starting with the paired CIS panels, backside insulation is found to negatively impact efficiency. The uninsulated CIS panel recorded an annual conversion efficiency of 10.2 % versus 9.7 % for the insulated equivalent. For the 2-a-Si panels, by comparison, the backside insulation had no appreciable effect; the annual conversion efficiencies were identical at 4.6 %.

A comparison of the three custom-made panels having the same poly-Si PV cells shows the range of performance that may be realized in constructing a BIPV panel with a very thin glazing, in this case the 0.05 mm polymers ETFE and PVDF, as opposed to using a comparatively thick 6 mm glass front cover. Based on coverage area, the polymer-front panels yielded annual efficiencies of 12.2 % versus 11.2 % for the glass-front equivalent panel. A comparison of this same insulated glass front panel and the test station A panel, which are identical except for the PV cell type, shows that the square poly-Si cells and the octagonal mono-Si cells have approximately the same cell conversion efficiencies, 11.6 % and 11.5 %, respectively. Because the poly-Si cells do not create any inactive voids, however, the test station B panel provides more PV area, and thus generates more power than the test station A mono-Si panel. This difference is reflected by the coverage area efficiencies: 11.2 % versus 10.1 %. Finally, a comparison of the newer CIS technology and the more established mono-Si technology provides some encouraging results for the thin film product. The 9.7 % annual conversion efficiency of the insulated CIS panel approached the 10.1 % value posted by the insulated mono-Si panel. Uncertainties associated with these annual conversion efficiencies and other reported parameters are listed in Appendix A.

Table 2 lists the percentage differences in power generation for the five most comparable cases. Results based on the two chosen data collection intervals are reported. The gain achieved by using the thin polymer front covers, as

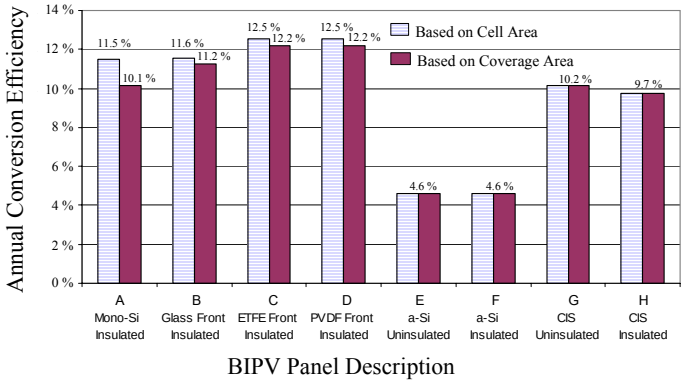


**Fig. 3 Annual Conversion Efficiencies for the Sunrise-to-Sunset Interval**

opposed to the 6 mm glass, is shown to fall between 7.8 % and 8.7 % based on the midday interval data and between 8.4 % and 8.6 % based on the sunrise-to-sunset interval data. As noted above, adding insulation to the 2-a-Si panel had no appreciable affect, with the percent difference changing sign between the two data collection intervals. The annual energy generation of the insulated CIS panel trailed by 4.2 % and 5.1 %, the latter corresponding to the midday interval.

Referring again to Table 2, the results suggest that the ETFE-front panel has a slightly different performance trend over the day, as compared to the PVDF- and glass-front panels. For example, the ETFE panel matches the performance of the PVDF panel when compared using data from the entire day but lags slightly when compared based on midday data. A plot of the difference in power production between the two polymer-front panels (i.e., PVDF – ETFE) on a clear day better demonstrates the subtle difference in performance, Fig. 4. This subtle difference in performance may be a function of panel temperature, angle of incidence, solar transmittance, or some combination. The degree to which the PVDF panel runs cooler than the ETFE panel (i.e., $T_{PVDF} - T_{ETFE} < 0$) is plotted in Fig. 4, along with the normalized solar irradiance over the day. The peak, plane-of-BIPV-panel (POP) irradiance on the chosen day was 682 W/m$^2$; the peak panel temperature for the hotter running ETFE panel was 43.0 °C. The authors plan to further investigate these and other performance differences in a separate technical paper that focuses exclusively on the effects of the three front cover materials.

The effect of the backside insulation on the CIS panels is shown in Figs. 5 and 6. Figure 5 plots the panel temperatures and power outputs of the paired CIS panels on a clear day. The backside insulation caused the panel to operate at a higher temperature than the uninsulated panel for the bulk of the daylight period. For this day in May, the peak temperature achieved by the insulated CIS panel was 51.5 °C, versus a 40.4 °C peak temperature for the uninsulated panel. These peak temperatures were achieved when the outdoor ambient temperature was 23.5 °C. The higher operating temperature caused degradation in the power output. This degradation was reflected in the operating voltage, Fig. 6. Whereas the operating currents of the two CIS panels were almost identical throughout the day (plot not provided), the operating voltages separated in a manner consistent with the separation of the operating temperatures. These results are expected because the thin-film CIS technology shares the same characteristic as

**Table 2. Percent Differences in Annual Energy Production**

| Data Interval | Front Cover Improvement: | | | Change Due to Backside Insulation | |
|---|---|---|---|---|---|
| | ETFE Versus Glass (%) | PVDF Versus Glass (%) | PVDF Versus ETFE (%) | 2-a-Si Panels (%) | CIS Panels (%) |
| Sunrise-to-Sunset | 8.4 | 8.6 | 0.1 | 0.1 | -4.2 |
| 2-a-Si Midday | 7.8 | 8.7 | 0.9 | -0.3 | -5.1 |

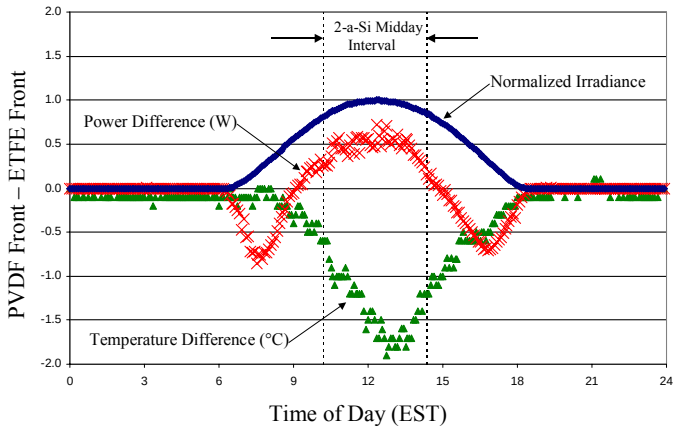


**Fig. 4 Performance Comparison: PVDF Versus ETFE Front Covers (March 23, 2002)**

crystalline silicon technologies: elevated operating temperatures affect voltage more than current. The earlier noted difference in the Table 2 values for the CIS panels is also understood given the greater likelihood of the gap in operating temperatures (in favor of the insulated panel) being greatest during the midday interval.

As noted earlier, the power production of the paired 2-a-Si BIPV panels tract each other closely, especially once the correction is applied to negate the effect of the inherit differences in the panels themselves. Figure 7 exemplifies the agreement, with the daily energy values for the insulated and uninsulated panels lying virtually on top of one another for the two selected months, June and November. The good agreement was independent of the selected data collection interval. The June data in Fig. 7 correspond to the results from the longer sunrise- to-sunset interval; the November data correspond to the shorter, 2-a-Si midday interval.

Figure 7 provides insight into the seasonal energy production for all of the vertically installed panels. Even with the November data in Fig. 7 being taken from the shorter midday data collection interval – an average duration of 6.0 hours per day – the energy generated on the better November days is approximately twice the energy production on the better June days. The fact that the vertical, south-facing BIPV panels do poorly at harvesting the bountiful solar resource available on those longer June days (with an average sunrise-to-sunset

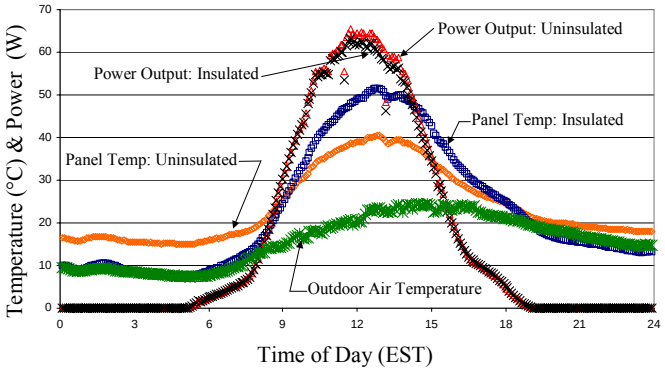


**Fig. 5 CIS Panels: Power Outputs and Operating Temperatures (May 5, 2002)**

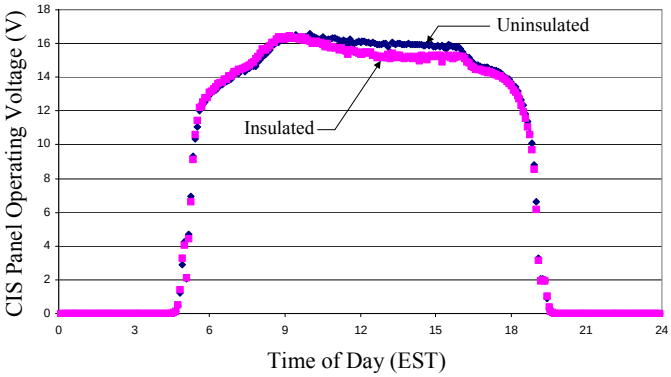


**Fig. 6 CIS Panels: Operating Voltages (May 5, 2002)**

interval of 14.7 h for NIST's latitude) is clearly shown by Fig. 7-type comparisons. In June, the vertical panels only "see" the sun for a relatively small interval at midday, and then, at very high angles of incidence. High angles of incidence themselves work against efficient PV energy production and, when combined with building and module framing components, promote shading (refer to Fig. 2).

It is worth noting that, when the average or overall energy production during the 30 d of June and the 30 d of November are compared – at least for the NIST test facility in 2002 – the differences in performance are not nearly as striking. As shown in Fig. 7, the local NIST weather in November 2002 was far more variable than June 2002, the latter having comparatively fewer mostly cloudy or overcast days. The total energy produced by all eight BIPV panels in November only exceeded the total output in June by 23.5 %; the better June weather partially compensated for the panel orientation effect.

Although the energy production of the 2-a-Si panel was not measurably affected by the higher operating temperatures created by the backside insulation, the operating voltages and currents of the paired 2-a-Si panels were minimally affected by panel temperature. The effect was more difficult to isolate because of the operating differences observed during the baseline periods when both panels were uninsulated. A correction, as applied to the power output, was not pursued with regard to voltage and current. Fortunately, the inherent performance difference in the paired 2-a-Si panels was worst at

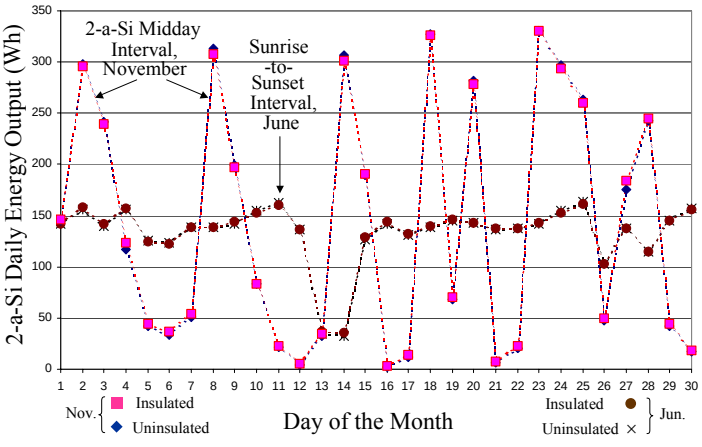


**Fig. 7 Daily Energy Production for the Paired 2-a-Si Panels: (1) Based on the Midday Data From November and (2) Based on the Sunrise-to-Sunset Data From June**

the lowest irradiances and became insignificant at irradiances of 600 W/m$^2$ and higher. The maximum power point currents and voltages plus the IV curves traced during the baseline periods were nearly identical matches for the highest irradiances. However, when the test station F panel was insulated, its open circuit and maximum power point voltages decreased slightly relative to the values recorded for the test station E panel. Conversely, the short circuit and maximum power point currents of the insulated panel moved slightly higher than those of the uninsulated panel. Figure 8 shows this offsetting effect of temperature. The IV curves at each irradiance, 628 W/m$^2$ and 816 W/m$^2$, were traced one after the other. The maximum power point for each curve is projected to the axes in an effort to better show the relative change in voltage and current. The results can be used to provide a first approximation as to the temperature coefficients for the 2-a-Si temperature panels:

- maximum-power current: +0.0021 A/°C
- short-circuit current: +0.0012 A/°C
- maximum-power voltage: -0.20 V/°C
- open-circuit voltage: -0.30 V/°C

These approximated temperature coefficients cannot be directly compared to the values typically reported in the literature because, especially with regard to the temperature coefficients for current, the values have not been normalized to standard rating conditions. No attempt at normalization is made here.

Although crude in approximating temperature coefficients, the long-term test facility can be helpful in another modeling related area: quantifying the departure in approximating the PV cells operating temperature based on the backside temperature of the PV panel or module. The custom-made panels in test stations A to D provide both temperature measurements. When the panels are insulated, as expected, the two temperature measurements track very closely, especially for the two glass-front panels where only the backsheet separates the two temperature sensors. The glass-front also acts to dampen the effect of changing convective heat transfer due to wind speed changes. During the daylight periods of Round 2, the difference in the temperatures measured by the embedded and backside thermocouples fell within the -0.5 °C to +0.5 °C range nearly 100 % of the time for the glass-front panels while roughly 97 % of the temperature differences for the polymer-front panels fell within ±1.0 °C. Based on measurements made when these same panels, as well as similar panels that were tested during the Round 1 study, were not insulated – as during the Round 2 baseline periods – the difference between the

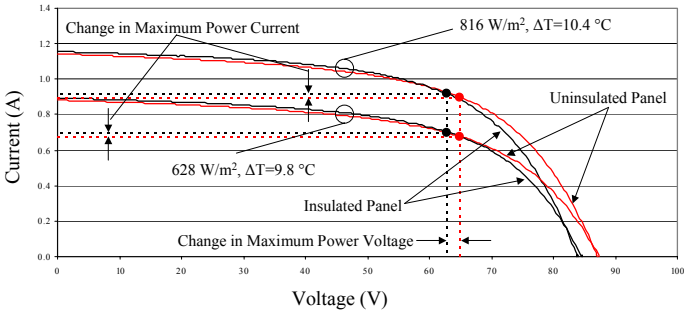


**Figure 8 Characteristic IV Curves for the Paired 2-a-Si Panels (November 2, 2002)**

embedded and backside temperature measurements would peak at a value less than 4 °C on the sunniest days. For this uninsulated case, no trend was observed as to the rank ordering of the temperature differences for the glass-front panels versus the polymer-front panels. Even though the two thermocouples for the polymer-front panels were separated by the backsheet, EVA, and 6 mm of glass, a plot of their daily temperature difference was very comparable to the plot recorded for the glass-front panels. These results show that cell temperature can be reasonably approximated by measuring the panel's backside surface temperature.

Returning finally to the issue of seasonal variations that was noted as part of the discussion of Figure 7, all eight BIPV panels performed better during the fall and winter versus the spring and summer. As shown in Figure 9, both 2-a-Si panels yielded a monthly coverage-area efficiency that peaked at 4.8 % in February and March versus registering a minimum of 4.3 % for June. The poly-Si panel having the PVDF front cover showed the greatest seasonal dependency, going from a high of 13.0 % for December to a low of 11.1 % for July. The two other poly-Si panels were only slightly less affected with the monthly percentages varying by the same absolute amount: 11.2 % to 12.9 % for the ETFE-front panel and 10.3 % to 12.0 % for the glass-front panel. The maximum changes in the percentages for the three other panels matched or approached this same absolute change, from 1.4 % (9.4 % to 10.8 %) for the mono-Si panel to 1.7 % for the uninsulated CIS panel (9.1 % to 10.8 %).

The seasonal variation is not attributed to panel operating temperature. During the midday interval when the panels generate the most energy, the panels temperatures recorded during the spring and summer months are lower than those obtained during the fall and winter months. For example, the peak backside panel temperature recorded for the ETFE front cover panel during January was 72.3 °C as compared to a 56.0 °C peak temperature for June.

The seasonal variation is instead attributed mainly to an angle of incidence (AOI) effect. For the vertical panels, significantly higher angles of incidence occur over a summer day versus a winter day [7]. For example, the AOI on the summer solstice at solar noon is 74.3° at the NIST test facility. By comparison, the AOI at solar noon on the winter solstice is 27.4° . Based on short-term characterization tests on comparable photovoltaic panels [5,10], reflectance losses typically begin at angles of incidence around 50°, increase gradually until the AOI is 60° to 65°, and then accelerate as the AOI approaches 90°. The longer daily intervals at angles of incidence of 50° and higher during the spring and summer caused the AOI effect on PV power generation to be more pronounced.

Two other factors that influenced the shape of the Fig. 9 plots are solar spectrum and irradiance. The relationship between solar spectrum and power generation differs among the different PV technologies. Some PV technologies, for example, do better at converting energy from the blue-end of the solar spectrum while others are more tuned for the red end of the spectrum. Prior testing and modeling of PV panels – where air mass is used to approximate solar spectrum variations – suggest that amorphous silicon panels do better during the spring and summer months (lower midday air masses) than

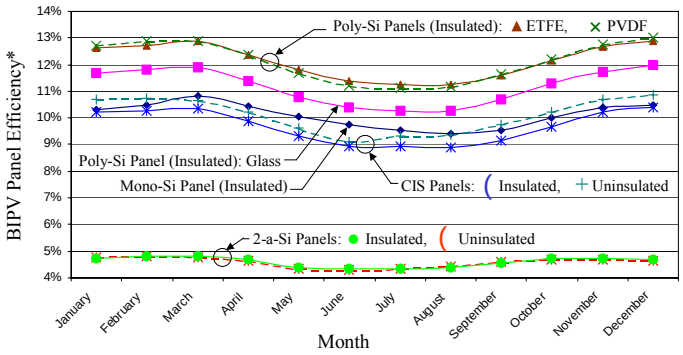


**Figure 9 Seasonal Variation in Coverage-Area Conversion Efficiency Based on the Sunrise-to-Sunset Data Interval**

during the fall and winter months (higher midday air masses), everything else being constant [5,10]. Crystalline panels, by comparison, are affected less by changes in solar spectrum and in an opposite manner; they do slightly better when exposed to the solar spectrum changes that are characteristic of days in fall and winter. For the 2-a-Si panels, the solar spectrum effect partly counter-acts the AOI effect, thus contributing to a smaller month-to-month variation (Fig. 9). For the other panels, the spectrum effect adds slightly to the AOI effect.

The daily range for the POP irradiances changes significantly over the year. For example, the peak POP irradiance on a clear day near the winter solstice is more than double the peak value for a clear day near the summer solstice. Based on data published in references 10 and 11, most PV technologies yield conversion efficiencies that change little for irradiances of 400 W/m$^2$ and higher while dropping off at differing rates at the lowest irradiances. Amorphous silicon modules, however, deviate from this general trend; their conversion efficiency is slightly greater at the lower and middle irradiances than at the highest irradiances. If the Round 2 panels have similar characteristics, the irradiance effect would partly counter-act the AOI seasonal effect for the 2-a-Si panels while again adding to the AOI seasonal effect for the other six BIPV panels.

## DISCUSSION AND CONCLUSIONS

The long-term testing of the Round 2 BIPV panels shows that a considerable performance improvement can be gained as the result of the front cover material (panel glazing). The study included materials that should bracket the range of possible options that could be considered. In one case, results are presented for custom-made BIPV panels that use 6 mm thick, low-iron float glass as the front cover. On the other extreme, results are presented for two very thin polymer front covers, each having a nominal thickness of 0.05 mm or 120 times thinner than the glass alternative. On an annual basis, the polymer front-cover panels provided 8.5 % more energy production than the glass-front panel. Flash testing on a separate set of similarly constructed panels shows similar rank ordering but only a 4.6 % difference (Table 1). Short-term solar tracker testing that quantify the effects of angle of incidence and air mass is nearing completion and tests of the glazing materials alone to get their optical properties are being pursued. Once these pieces of information are collected, the authors plan to write a paper that focuses on this front cover

effect. Because of the relatively short-term nature of this study, data addressing whether the optical properties of the polymer front covers degrade over time is not available.

Although slightly masked by their use within the panels having the three different front covers, the performance of the wafer-type polycrystalline cells tested in Round 2 was impressive. The glass-front BIPV panel having the poly-Si cells yielded an annual cell area conversion efficiency that effectively matched the otherwise similarly constructed BIPV panel having mono-Si cells. The poly-Si cells are square whereas the mono-Si cells are octagonal shaped and, for this study, both had the same nominal 125 mm size. The larger actual cell area of the poly-Si cells results in more power production per cell and a more efficient layout within a BIPV panel. When compared on the basis of annual coverage-area efficiency, where this difference in cell shape is accounted, the glass-front poly-Si panel bettered the mono-Si equivalent panel, 11.2 % versus 10.1 %. As a reminder, these numbers reflect a conservative situation. All the BIPV panels were oriented vertically and these two panels plus four of the six other Round 2 panels were well insulated on their backsides. Even better performance would be expected if these BIPV panel were applied at a lower tilt and/or (with the exception of the 2-a-Si panel) installed without the backside insulation.

The energy production of the BIPV panels created using two parallel–wired, tandem junction amorphous silicon modules was negligibly affected by the addition of backside insulation. The insulation caused the panel to run hotter during the midday, higher insolation periods. The maximum power point and the IV curve trace shifted slightly, relative to those of the uninsulated 2-a-Si panel, during these times. The higher operating temperature caused the maximum power and open circuit voltages to decrease and the maximum power and short circuit currents to increase (Fig. 8). The directions of these shifts are consistent with the published data [12]. However, the offsetting effect observed in this study in not consistent with findings reported by others that have studied the performance of amorphous silicon products [12,13]. These researchers reported an overall negative effect on power output as panel temperature increases. As conveyed in Reference 13, understanding the performance characteristics of amorphous silicon products has been somewhat elusive and thus a subject for continued discussion.

As compared to the 2-a-Si panel, backside insulation was observed to negatively affect the power production of the CIS panel. On an annual basis, the insulated CIS panel produced 4.2 % less energy than the uninsulated CIS panel. The difference in operating temperatures between the two panels did not have a measurable impact on the maximum power current. Maximum power voltage, by comparison, had a temperature dependency, one that was comparable to crystalline PV products.

As for a brief status report, year-long monitoring of a third set of BIPV panels in the same NIST test facility commenced on January 1, 2004. The Round 2 BIPV panels have been characterized sufficiently using the solar tracker to move forward with comparing their predicted performance with the measured, year-long performance. A mini round robin is underway with the same panels tested at NIST being tested by researchers at the Sandia National Laboratories.

## ACKNOWLEDGMENTS

The project was partially funded by the Premium Power Focus Program that is managed by the NIST Advanced Technology Program (ATP). The authors thank ATP's Gerry Ceasar for championing this research. Gerry's knowledge, sincere interest, and positive attitude contribute to the success of the project. A few notable PV industry members who assisted this second round of BIPV testing include David Meakin, Clin Lashway, Jake Brown, and Pete DeNapoli. David was instrumental in having custom-length, BP Solar 2-a-Si modules donated to NIST for testing; David was extremely helpful in answering installation questions and interpreting some of the 2-a-Si panel test results. Clin supported us with rare but timely repairs, calibration services, and answers to questions tied to operating the photovoltaic multi-tracer. Jake oversaw the fabrication of the Round 2 custom-made BIPV panels having the different front covers and was always willing to discuss technical issues tied to his product. Pete DeNapoli was always willing to discuss his products and our research and solicit colleagues for information on our behalf.

The authors acknowledge NIST coworkers Luis Luyo and Paula Svincek, NIST coop students David Frankford and Andrew Heath, and NIST contractor Merle Guyton. Merle fabricated the composite 2-a-Si and CIS BIPV panels and routed the foam insulation to provide a custom fit to the backside of the Round 2 insulated panels. David assisted with instrumenting the Round 2 panels and getting the year-long project started. Luis and Andrew helped at the project's end, both in transitioning to the Round 3 panels and in reducing the very large amount of Round 2 data. Paula supports the authors and this project in many ways. Her administrative and secretarial talents made this project and this paper's development, review, and final preparation a lot less burdensome for the authors.

## APPENDIX A

Expanded uncertainties (k=2) of reported quantities are provided in Table 3. These uncertainties were calculated using current international guidelines [14]. An uncertainty for the integrated BIPV panel power (i.e., energy) and integrated solar irradiance are not reported in the table because their relative uncertainties become negligible due to the large number of individual measurements that are summed over the day, month, and year. Instead, the uncertainties of the corresponding individual measurements are listed. Finally, the uncertainties for panel voltage, panel current, and the primary panel power are based on the poorest match between the BIPV panel's electrical characteristics and the multi-tracer (and its unique range levels and accuracy for each range). For example, the voltage, current, and primary power uncertainties correspond to panels in the following test stations, respectively: A to D, E and F, and A.

| Table 3. Expanded Uncertainties of Primary Measurements | |
|---|---|
| Quantity | Expanded (k=2) Uncertainty (%)[1] |
| BIPV Panel Power – primary[2] | 0.73 |
| BIPV Panel Power – secondary[3] | 1.0 |
| BIPV Panel Voltage | 0.46 |
| BIPV Panel Current | 0.81 |
| Solar Irradiance | 2.3 |
| BIPV Panel Conversion Efficiency[4] | 2.5 |
| BIPV Panel Area | 0.31 |
| BIPV Panel Temperature | 0.22 |

[1]The expanded uncertainty for panel temperature is expressed in units of degrees Celsius.
[2]Measurents made using the multi-tracer instrument.
[3]Measurements made using the redundant digital power meter used only in test station D.
[4]Listed value based on using instantaneous BIPV panel power and solar irradiance measurements; uncertainties for the monthly and yearly efficiencies approach the uncertainty of the BIPV panel area.

## REFERENCES


[1] Davis, M. W., Fanney, A. H., and Dougherty, B. P., 2002, "Evaluating Building Integrated Photovoltaic Performance Models," Proceedings of the 29th IEEE Photovoltaic Specialists Conference, New Orleans, LA, pp. 1642-1645.

[2] PHotovoltaic ANalysis and TrAnsient Simulation Method (PHANTASM), 1999, Building Integrated Photovoltaic Simulation Software, Solar Energy Laboratory, University of Wisconsin, Madison, WI.

[3] King, D. L., Boyson, W. E., and Kratochvil, J. A., "Photovoltaic Array Performance Model," Sandia Report SAND2004-3535, Sandia National Laboratories, August 2004.

[4] Ransome, S. and Wohlgemuth, J., 2002, "Understanding and Correcting kWh/kWp Measurements," Proceedings of the 18th European Photovoltaic Solar Energy Conference, Rome, OE6.2.

[5] Fanney, A. H., Dougherty, B. P., and Davis, M. W., 2003, "Short-Term Characterization of Building Integrated Photovoltaic Panels," ASME Journal of Solar Energy Engineering, Vol. 125, pp. 13-20.

[6] King, D. L., Kratochvil, J. A., and Boyson, W. E., 1998, "Field Experience with a New Performance Characterization Procedure for Photovoltaic Arrays," Proceedings of the 2nd World Conference and Exhibition on Photovoltaic Solar Energy Conversion, Vienna, Austria.

[7] Fanney, A. H., Dougherty, B. P., and Davis, M. W., 2001, "Measured Performance of Building Integrated Photovoltaic Panels," ASME Journal of Solar Energy Engineering, Vol. 123, pp. 187-193.

[8] Fanney, A. H., Dougherty, B. P., 2001, "Building Integrated Photovoltaic Test Facility," ASME Journal of Solar Energy Engineering, Vol. 123, pp. 194-199.

[9] Meakin, D., previously with BP Solar, Toano, Virginia, private phone and email communications, April 8-10, 2003.

[10] King, D. L., Boyson, W. E., 2002, and Kratockvil, J. A., "Analysis of Factors Influencing the Annual Energy Production of Photovoltaic Systems," Proceedings of the 29th IEEE Photovoltaic Specialists Conference, pp. 1356-1361.

[11] Eikelboom, J. A. and Jansen, M. J., 2000, "Characterisation of PV Modules of New Generations: Results of Tests and Simulations," ECN-D-00-067, Energy Research Centre of the Netherlands, July.

[12] King, D. L., Kratockvil, J. A., and Boyson, W. E., 2000, "Stabilization and Performance Characteristics of Commercial Amorphous-Silicon PV Modules," Proceedings of the 28th IEEE Photovoltaic Specialists Conference, September, pp. 1446-1449.

[13] Wohlgemuth, J. H. and Ransome, S. J., 2002, "Performance of BP Solar Tandem Junction Amorphous Silicon Modules," Proceedings of the 29th IEEE Photovoltaic Specialists Conference, May, pp. 1142-1145.

[14] ANSI, 1997, "U.S. Guide to the Expression of Uncertainty in Measurement," ANSI/NCSL Z540-2-1997.